國立交通大學

物理研究所

碩 士 論 文

來自伽瑪射線爆之微中子

Neutrinos from gamma-ray burst

研 究 生：周禹廷

指導教授：林貴林　教授

中 華 民 國 一百 年 一 月

來自伽瑪射線爆之微中子
Neutrinos from gamma-ray burst

研 究 生：周禹廷　　Student：Yu-Ting Chou

指導教授：林貴林　　Advisor：Guey-lin Lin

國 立 交 通 大 學

物理研究所

碩 士 論 文

A Thesis

Submitted to Institute of Physics

College of Science

National Chiao Tung University

in partial Fulfillment of the Requirements

for the Degree of

Master

in

Physics

January 2011

Hsinchu, Taiwan, Republic of China

中華民國一百年一月

來自伽瑪射線爆之微中子

學生：周禹廷　　指導教授：林貴林

國立交通大學物理研究所碩士班

摘　　要

本論文研究來自伽瑪射線爆的微中子其流量以及味組成，首先考慮典型的伽瑪射線爆。其次計算不同磁場大小對微中子流量以及味組成的影響，並探討流量以及味分布以及與不同光學能譜之伽瑪射線爆之關連性。我們主要探討是否有純粹由中子衰變的微中子流。動機來自於 Mohara and Gupta 發表的研究。我們的結果將與 Mohara 此篇作比較。

Neutrinos from gamma-ray burst

student：Yu-Ting Chou Advisors：Dr. Guey-Lin Lin

Institute of Physics
National Chiao Tung University

ABSTRACT

In this thesis we predict the neutrino flux and flavor composition from gamma-ray bursts (GRBs). At first we consider typical gamma-ray bursts. We calculate the magnetic field effects on GRBs with different magnetic field strength. We also consider the flux and flavor composition dependencies on photon spectra indices for different gamma ray bursts. We aim to look for a pure neutron beam. This thesis is motivated by a study by Moharana and Gupta. We compare our result with that of Moharana and Gupta.

誌　　謝

這篇論文的完成，首先感謝指導教授林貴林老師，老師不僅給了我極大自由去尋找方向，同時也嚴謹和細心地探討其中的物理以及耐心修改這篇論文，在這段時間內也感受到了老師的關心還有包容。謝謝兩位口試委員高文芳教授以及賴光昶教授，兩位老師的意見還有問題都對論文的修改大有裨益。在文字處理排版方面，謝謝單中林博士之前在 LATEX 以及 Beamer 使用上的一些教學。同時致謝臺灣大學的陳志清學長，在我碩士生涯參與的幾個問題裡都給了很大的幫助。

謝謝我們的研究團隊中的王正祥老師、黃明輝老師、宗哲學長、永順學長、貝禎學姐、佳均學姊、志榮同學、念潔同學、互相討論駁難，諸位也解答了我這個問題兒童不少的問題。

碩士班生涯中交到了很多好朋友，謝謝德明學長、平翰學長、宏慶學長、琳元同學以及許多同學和學弟妹給予許多生活上的建議、娛樂還有聽我訴苦。

謝謝父母一直在物質上及精神上支持我的學業，這篇論文是微薄的成就，不足以報答萬分之一。

最後的感謝留給讀者，你的閱讀賦予了這篇論文意義。

Contents

List of Figures

List of Tables

Chapter 0

Introduction

Neutrinos are generated by photon interacting with proton in the universe. These neutrinos are so-called astrophysical neutrinos. Astrophysical neutrinos have different flavor compositions, and flavor compositions could change from the source to the earth. Different gamma-ray burst(GRB) and active galactic nuclei (AGN) models are proposed to be the leading source candidates to accelerate the protons and hence produce neutrinos. The neutrino detection will be the key to verify these astrophysical models.

In this thesis we predict the neutrino fluxes and flavor compositions before oscillation from gamma-ray bursts. We first consider typical gamma-ray bursts. We then focus on the magnetic field effects and the dependence on observed photon spectra indices from different kinds of gamma ray bursts.

We are motivated by a study by Moharana and Gupta [28]. Moharana and Gupta suggest a pure neutron beam source (pure (anti-)electron-neutrino before oscillation) from typical gamma-ray bursts. They argued that such beams were caused by the magnetic field synchrotron effects on pion [28]. However this argument is not self-consistent in our view. We will discuss the problems and compare our result with that of Ref. [28].

In Chapter 1, we introduce the ultra high energy cosmic ray, the possible acceleration mechanism and possible astrophysical source candidates. In Chapter 2, we discuss the astrophysical neutrino production. We discuss the basic interactions and the possibility of neutrino fluxes coming from Active galactic nucleus and gamma-ray burst. We argue that gamma-ray burst is the more probable source. In Chapter 3, we review the gamma ray burst model and introduce the method for calculating neutrino flux. We set the magnetic field strength and the index of photon spectrum as the main parameters in general GRBs. We then discuss special GRB source and look for a pure neutron beam source. Quantitative results such as predicted fluxes on Earth are presented in Chapter 3 as well. Chapter 4 is the conclusion.

Chapter 1

Ultra high energy cosmic ray

Ultra high energy cosmic rays (UHECRs), are particles from universe with very high energies, up to 10^{20} eV. UHECR has been an important research topic since 1950's, after the constructions of Volcano Ranch (USA) and Moscow University (USSR) arrays. At present, data from Yakutsk [15], AGASA [6, 14], HiRes [24], and Pierre Auger [18] confirm an observed power law spectrum $\frac{dI}{d\mathcal{E}} \propto \mathcal{E}^{-\alpha_{ob}}$ with $\alpha_{ob} \simeq 2.7$ of the flux in the main energy region ($\mathcal{E} < 5 \times 10^{19}$ eV).

Since the energies of these particles are very high, it is natural to ask: what is the acceleration mechanism and what are the origins of the UHECRs. Extensions of Fermi acceleration mechanism can explain the acceleration mechanism. Gamma-ray bursts and active-galactic nuclei models are the leading source candidates. Neutrinos flux and flavor compositions may be the key to verify these models. Our main concern is the neutrinos coming from gamma-ray burst.

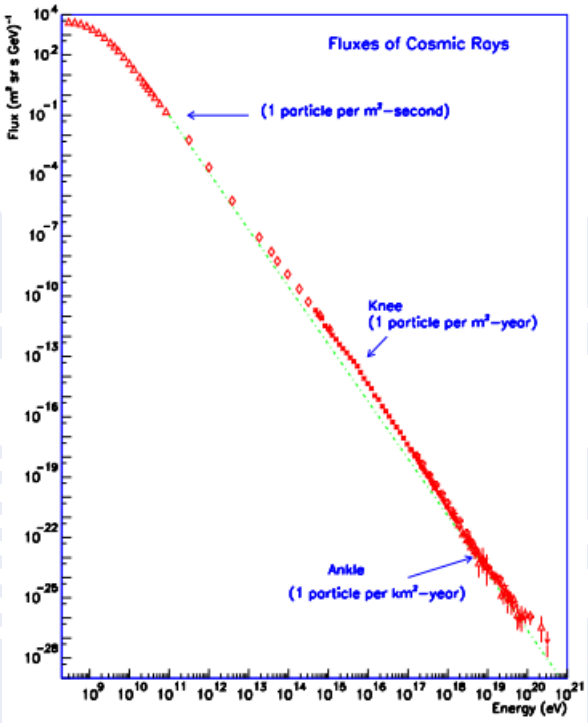

Figure 1.1: The cosmic ray spectrum expands 12 decades of energies. This figure is assembled by several measurements [9, 17].

1.1 Fermi acceleration mechanism

Fermi (1949) constructed the basic acceleration mechanism of UHECR [1]. He argued that charged particles can be accelerated when reflected by a magnetic mirror. This is thought to be the primary mechanism by which particles gain energy beyond the thermal energy in astrophysical shock waves. The basic model was constructed with a non-relativistic shock. Fermi's theory was extended for a relativistic shock [4], which can be applied to explain GRBs and AGNs as the origins of UHECR. The resulting energy spectrum of this process (assuming that they do not influence the structure of the shock) turns out to be a power law spectrum $\frac{dI}{d\mathcal{E}} \propto \mathcal{E}^{-\alpha_{so}}$ with $\alpha_{so} \simeq 2.0 - 2.3$ at the

sources. Some diffusing models [22] can accont for α_{ob} becoming $\simeq 2.7$ after cosmological evolutions of UHECR are considered.

1.2 The origin of UHECR

The origin of UHECR is one of the most exciting questions in high energy astrophysics. It is a challenge to model the acceleration of highest energy particles in astrophysical sources. Among many proposed models, gamma-ray bursts (GRBs) and active galactic nuclei(AGNs) are the most prominent candidate sources of the UHECR [22, 19]. The protons (or heavy nuclei) in these objects are typically assumed to be accelerated in the relativistic outflow together with electrons and positrons by Fermi shock acceleration. The accelerated protons interact with photons, leading to the production of neutrinos.

1.2.1 Gamma-ray burst

Gamma-ray bursts(GRBs), first observed in the late 1960s by the U.S. Vela satellites, are flashes of ($\sim$ 10 keV to $\sim$ 100 MeV) photons.

At first GRB was thought to be nearby sources within the Milky Way Galaxy. The Burst and Transient Source Experiment (BATSE [12, 13]) provided crucial data indicating that the distribution of GRBs is isotropic towards any particular direction in space, such as toward the galactic plane or the galactic center. Because of the flattened shape of the Milky Way Galaxy, sources within our own galaxy would be strongly concentrated in or near the galactic plane. The absence of such a pattern in GRBs provides a strong evidence that gamma-ray bursts must be a cosmological event coming from places beyond the Milky Way.

GRB is the most luminous photon flux ($\sim 10^{52}$ erg/s) explosions (if treated as cosmological events) known to occur in the universe. Bursts can last from 10ms to 1000s typically [21]. Several models for the origin of gamma-ray bursts postulated that the initial burst of gamma rays should be followed by slowly fading emission at longer wavelengths created by collisions between the burst ejecta and interstellar gas. This emission is so called the "afterglow". A long- duration burst ($\gtrsim$ 2s) is usually followed by a longer-lived "afterglow" which emits low-energy photons (X-ray, ultraviolet, optical, infrared and radio). On the contrary, no afterglow is detected from short-duration ($\lesssim$ 2s) bursts generally.

Related to the observations of afterglow, long bursts are believed to be associated with a rapidly star-forming galaxy. Short bursts are believed to be no star formation, including large elliptical galaxies and the interstellar medium.

The true nature of GRBs remains unknown. On the causes of gamma ray bursts, there is a speculation that GRB is produced by the merger of two compact objects such as neutron stars or black holes. Another view is that GRB is from the evolution of massive stars to the black hole. In 1998, a high-energy supernova SN1998bw, is discovered to be connected with the burst GRB980425. This relation between (long duration) GRBs with supernovae indicates a connection between GRBs and the deaths of very massive stars [11].

1.2.2 Active galactic nucleus

An active galactic nucleus (AGN) is a compact region at the centre of a galaxy. AGN has a higher luminosity ($\sim 10^{43} - 10^{48}$ erg/s) than the other part of the galaxy in almost all ranges of the electromagnetic spectrum. Such

excess emission has been observed in the radio, infrared, optical, ultra-violet, X-ray and gamma-ray wavebands. A galaxy hosting an AGN is called an active galaxy. The radiation from AGN is believed to be resulting from accretion of mass by the super massive black hole at the centre of the host galaxy.

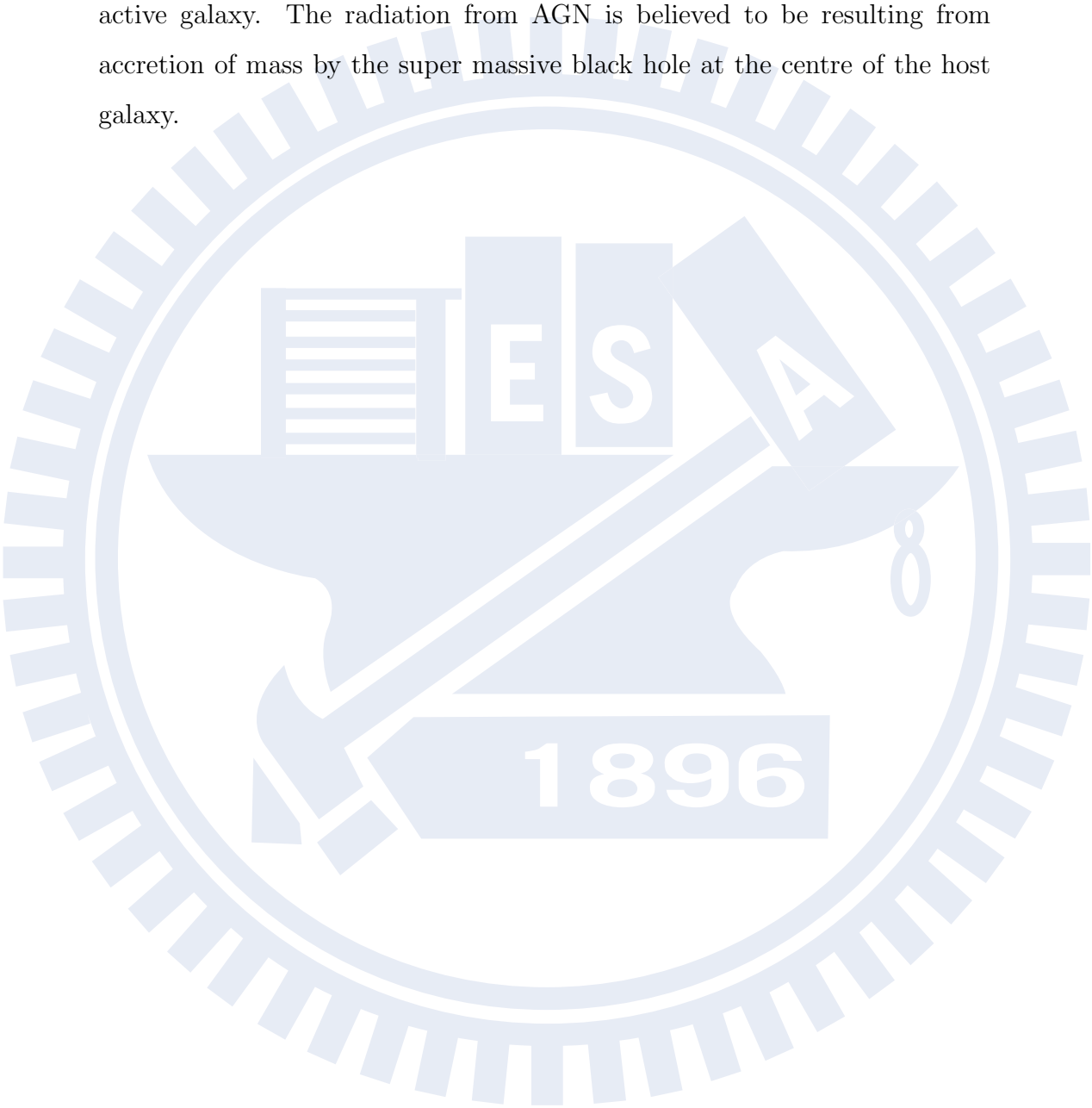

Chapter 2

Astrophysical neutrinos

2.1 Production of neutrinos

High energy neutrinos produced in astrophysical sources, are mainly coming from the photon-pion interaction. High energy protons and photons interact with each other via Δ^+ resonance

$$p + \gamma \to \Delta^+ \to p + \pi^0 \ . \tag{2.1}$$

$$p + \gamma \to \Delta^+ \to n + \pi^+ \ . \tag{2.2}$$

Neutrinos are produced by the decays of neutrons (beta decay) and charged pions in the scenario (2.2).

For the latter case, the secondary muon from pion decays can decay into an anti-muon neutrino and an electron-neutrino. Hence the pion decay chain is described by

$$\pi^+ \to \mu^+ + \nu_\mu \ , \tag{2.3}$$

and

$$\mu^+ \to e^+ + \nu_e + \bar{\nu_\mu} \ . \tag{2.4}$$

The neutron beta decay simply produce an anti-electron-neutrino, i.e.,

$$n \rightarrow p + e^{-} + \bar{\nu_e} \ . \tag{2.5}$$

2.2 GZK cutoff and GZK neutrinos

There is a cut-off in UHECR spectrum in the energy region $\mathcal{E} > 5 \times 10^{19}$ eV. This phenomena is possibly related to the 2.7K cosmic microwave background. Greisen, Zatsepin and Kuzmin proposed a model to explain the above-mentioned (GZK) cut-off of UHECR spectrum. They treated UHECR as protons, and considered their interactions with CMB photons as Eq.(2.1) and Eq.(2.2). Since the 2.7K photon is at the low energy, the proton energy should be higher than 5×10^{19}eV to reach the maximum cross-section at Δ-resonance. Such a threshold energy exactly corresponds to the cutoff of UHECR spectrum. The GZK neutrino flux is small and have not yet been detected. This model is controversial. Some theories (e.g. Berezinsky [25]) suggest an upper-limit on the acceleration of UHECR, and therefore the cut-off is caused by the acceleration limit, not by the interactions with CMB.

2.3 GRB and AGN neutrinos

As mentioned in Chapter 1, the leading candidates of UHECR are GRB and AGNs. The accelerated proton or nuclei may interact with photons in those sources as Eq.(2.1) and Eq. (2.2). Such interactions produce neutrinos. In the GRB fireball model, the observed gamma-rays are produced by synchrotron emission of the co-accelerated electrons in the expanding shock. The GRB neutrino production is our main subject, and will be discussed later in Chapter 3.

In AGN-jets models, AGN jets produce the observed gamma-ray background. Secondly, high energy photon emission is due to decays of neutral pions. The predicted neutrinos flux from AGN-jets models is higher than those of other source candidates (comparing with neutrinos from GRB for $\mathcal{E}_\nu > 10^{15}$eV).

2.4 The cosmic ray limit

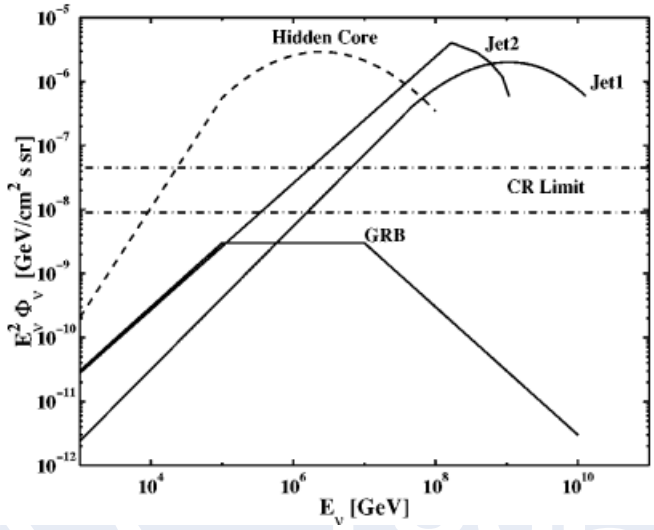

Figure 2.1: Comparison of the muon neutrino intensities [8] predicted by different models. The dash-dotted lines state the upper bound. The lower line is obtained by assuming no evolution, and the upper line assuming rapid evolution similar to the evolution of the quasi-stellar object.

To determine whether GRB or AGN is the dominating source of UHECR, Waxman and Bahcall derived a limit for predicted neutrino flux. This limit is derived from the injection spectrum of UHECR. Comparing each prediction, Waxman and Bahcall argued that GRB is a proper origin of UHECR,

because predicted neutrino flux from AGN-jets exceeds the limit by two orders of magnitude. In this case, one may try to observe the neutrinos in the GRB-dominating spectrum region ($\lesssim 10^{15} - 10^{16}$eV) instead of AGN-jets-dominating region ($\gtrsim 10^{15} - 10^{16}$eV). Differing from jets-model, a hidden core model in AGN, with proton photo-meson optical-depth, can not be limited by this bound.

This limit is controversial. Another limit suggest by Ref. [20] allows AGN-jets to be the dominating UHECR origin.

2.5 Neutrino flavor ratio at the astrophysical sources

Different astrophysical source may lead to different neutrino flavor ratio in different energy region. In the flavor ratio discussion we do not distinguish anti-neutrinos from neutrinos, but only distinguish the neutrino flavor.
The following typical classes of neutrino sources are considered:

Pion beam

Neutrinos are produced by the charged pion and secondary muon as Eq. (2.3) and (2.4), leading to a flavor ratio

$$\phi_{\nu_e} : \phi_{\nu_\mu} : \phi_{\nu_\tau} = 1 : 2 : 0 \ .$$

Muon damped source

In the magnetic field, charged pions and muons lose energies by synchrotron emission. Comparing synchrotron loss time scale and decay time scale for each particle, muons may lose energy before decay in some energy

region, while the same effect on pion is not obvious. This leads to a flavor ratio

$$\phi_{\nu_e} : \phi_{\nu_\mu} : \phi_{\nu_\tau} = 0 : 1 : 0 \ .$$

Neutron beam source

Anti-electron neutrinos from the neutron β-decay may be dominating in some cases. In the region that the synchrotron losses of the pions and muons are so large (i.e., the magnetic fields are very strong), relatively high energy neutrinos from neutron decays may give more important contributions.

On the other hand, depending to the photon spectra indices, one may find a neutron beam dominance in the low energy region as well. Another potential source of neutron beam is for photo-dissociation of heavy nuclei [26]. The flavor type of neutron beam is

$$\phi_{\nu_e} : \phi_{\nu_\mu} : \phi_{\nu_\tau} = 1 : 0 : 0 \ .$$

Mixed beam sources

In some energy region, neither the neutron beam source (1:0:0) or the pion beams (1:2:0) can be distinguished. The beam is mixed of the two. An example of a mixed beam is

$$\phi_{\nu_e} : \phi_{\nu_\mu} : \phi_{\nu_\tau} = 1 : 1.5 : 0 \ .$$

2.6 The neutrino oscillation

The neutrino flavor eigenstates (ν_e, ν_μ, ν_τ) are not identical to the mass eigenstates (defined as ν_1, ν_2, ν_3 commonly). This fact leads to the neutrino oscillation. For example, one may produce an electron-neutrino and find that

the electron neutrino could become a muon neutrino when making detection of this neutrino some distance from the production point.

For the oscillation of the astrophysical neutrinos, the initial flux $\phi^{(i)}_{\nu_x}$ (at astrophysical source) is related to the final flux $\phi^{(f)}_{\nu_x}$ (on earth) by the probability matrix P.

$$\begin{pmatrix} \phi^{(f)}_{\nu_e} \\ \phi^{(f)}_{\nu_\mu} \\ \phi^{(f)}_{\nu_\tau} \end{pmatrix} = P \begin{pmatrix} \phi^{(i)}_{\nu_e} \\ \phi^{(i)}_{\nu_\mu} \\ \phi^{(i)}_{\nu_\tau} \end{pmatrix} = \begin{pmatrix} P_{ee} & P_{\mu e} & P_{\tau e} \\ P_{e\mu} & P_{\mu\mu} & P_{\tau\mu} \\ P_{e\tau} & P_{\mu\tau} & P_{\tau\tau} \end{pmatrix} \begin{pmatrix} \phi^{(i)}_{\nu_e} \\ \phi^{(i)}_{\nu_\mu} \\ \phi^{(i)}_{\nu_\tau} \end{pmatrix} , \tag{2.6}$$

where P_{xy} is a simplified notation for the probability of flavor transition $P(\nu_x \to \nu_y)$. To simplify, the probability can be approximated by

$$P(\nu_x \to \nu_y) = \sum_i |U_{xi}|^2 |U_{yi}|^2 \tag{2.7}$$

within the condition that the oscillation lengths of the astrophysical sources neutrinos are averaged.

Here U is the Pontecorvo-Maki-Nagakawa-Sakata mixing matrix [7]

$$U = \begin{pmatrix} c_{12}c_{13} & s_{12}c_{13} & s_{13}e^{-i\delta} \\ -s_{12}c_{23} - c_{12}s_{23}s_{13}e^{i\delta} & c_{12}c_{23} - s_{12}s_{23}s_{13}e^{i\delta} & s_{23}c_{13} \\ s_{12}s_{23} - c_{12}c_{23}s_{13}e^{i\delta} & -c_{12}s_{23} - s_{12}c_{23}s_{13}e^{i\delta} & c_{23}c_{13} \end{pmatrix} \tag{2.8}$$

where $c_{ij} = \cos\theta_{ij}$, $s_{ij} = \sin\theta_{ij}$, and δ is the CP violating phase.

Chapter 3

Neutrinos from GRB

The frames

Here we use quantities with a prime $'$ in the GRB shock rest frame S', quantities with a star * in the GRB source centre frame S^*, and quantities without special marks in the observer's frame S. S^* relates to S' by a Lorentz boost factor Γ, while S relates S^* by a red-shift $(1+z)$. The red-shift z can be determined by the distance between GRB source and Earth. To simplify, we neglect the red-shift effect, i.e., $z = 0$. In this condition we can treat $S^* = S$.

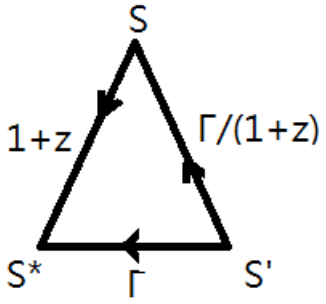

Figure 3.1: The relations of three frames

The calculations is based on models in Refs.[8, 10, 13, 19, 21, 28]. We use the formulae in SI units. The formulae may appear differently in these references due to different systems of unit employed.

3.1 Relativistic fireball

The GRB centre is a compact source of massive material. The leading model for the electromagnetic radiations observed from GRBs is based on the relativistic fireball created in the core collapse or merger. A gravitational collapse leads to the release of the ultimate high energy. The energies transform into $e^{\pm}$, gamma-rays and baryons expands relativistically, as a "fireball". The optical depth in the centre is very high. That leads to pair productions. The fireball expansions reduces the optical depth: If the fireball expands with a Lorentz factor Γ, the energy of photons in the fireball frame is relatively small, with a factor $1/\Gamma$, and therefore most photons may be below the pair production threshold. This consideration of the optical depth yields the lower limit of the Γ factor

$$\Gamma \gtrsim 100 \ .$$

As the fireball expands, a fireball shell could collides with another fireball shell. This collision leads to a (internal) relativistic shock. The protons are accelerated in the shock according to Fermi's model.

3.1.1 The total energy of internal shock

The acceleration region size r_i is constrained by the gamma factor and the variability time t_v (the time difference between each shell of the shock),

$$r_i \sim 2\Gamma^2 c t_v \ . \tag{3.1}$$

In this model the observed energy $\mathcal{E}_\gamma$ is from the synchrotron emission of the charged electrons and positrons. The electrons (positrons) take a fraction ξ_e of total energy of the shock L_{int} and transfers energy into the photon energy. We have $L_\gamma = \xi_e L_{int}$. The magnetic field takes a fraction ξ_B of the total energy.

$$\frac{2\pi r_i^2 c\Gamma^2 B'^2}{\mu_0} = \xi_B L_{int} = \frac{\xi_B L_\gamma}{\xi_e} \ . \tag{3.2}$$

There is an assumption that the fraction is equal-partitioned $\xi_e = \xi_B$. The value of each fraction can not be determined by any model. Following Refs. [13, 28] we choose

$$\xi_e = \xi_B = 0.3 \ .$$

3.1.2 The photon break energy

The GRB photon spectrum is fitted with the Burst and Transient Source Experiment (BATSE) data in the energy domain 20 keV to 2 MeV. The photon has a broken-power-law spectrum:

$$\mathcal{E}_\gamma \frac{dI_\gamma}{d\mathcal{E}_\gamma}(\mathcal{E}_\gamma) \propto \begin{cases} \mathcal{E}_\gamma^{-\alpha_1} & \text{if } \mathcal{E}_\gamma \leq \mathcal{E}_{\gamma,br} \\ \mathcal{E}_\gamma^{-\alpha_2} & \text{if } \mathcal{E}_\gamma \geq \mathcal{E}_{\gamma,br} \end{cases} , \tag{3.3}$$

where the indices $\alpha_1 \approx 0$, and α_2 can be up to 4. On the average, α_2 is between 1.0 and 1.2 . We note that, $\mathcal{E}_\gamma = \Gamma \mathcal{E}'_\gamma$.

The characteristic photon energy is determined by the strength of the magnetic field

$$\mathcal{E}'_\gamma = \frac{\hbar \Gamma_e^2 e B'}{m_e} \ , \tag{3.4}$$

which implies

$$\mathcal{E}_\gamma = \frac{\Gamma \hbar \Gamma_e^2 e B'}{m_e} \ . \tag{3.5}$$

where $\Gamma_e \approx \xi_e (m_p/m_e)$ is the Lorentz factor of electron-comoving frame relative to the shock frame.

3.2 Prediction of the neutrino spectrum from GRB

3.2.1 The spectrum of proton

In the calculation of the neutrino spectrum, the maximum energies of π, n, ν_μ, ν_e are all constrained by the maximal proton energy $\mathcal{E}_{p,max}$. Hümmer *et al.* [23] suggest the following proton spectrum:

$$\frac{dI_p}{d\mathcal{E}_p}(\mathcal{E}_p) \propto \begin{cases} \mathcal{E}_p^{-2} & \text{if } \mathcal{E}_p \leq \mathcal{E}_{p,max} \\ 0 & \text{if } \mathcal{E}_p \geq \mathcal{E}_{p,max} \end{cases} , \tag{3.6}$$

which has an artificial step function cut-off in the energy spectrum.
The step function is not realistic in our view. We consider a proton spectrum which is exponentially suppressed after the maximum energy,

$$\frac{dI_p}{d\mathcal{E}_p}(\mathcal{E}_p) \propto \begin{cases} \mathcal{E}_p^{-2} & \text{if } \mathcal{E}_p \leq \mathcal{E}_{p,max} \\ \exp(-\frac{\mathcal{E}_p}{\mathcal{E}_{p,max}}) & \text{if } \mathcal{E}_p \geq \mathcal{E}_{p,max} \end{cases} . \tag{3.7}$$

Eq. (3.7) is employed by Ref. [20].

The maximum of proton energy

The above mentioned maximum energy in the observer's frame relates to a maximum in the shock frame. In the case that the red-shift effect is negligible, we have

$$\mathcal{E}_{p,max} = \Gamma \mathcal{E}'_{p,max} .$$

The maximal proton energy in the shock frame can be derived by comparing the acceleration time t'_{acc} and the proton synchrotron loss time t'_{sync} of proton.

The acceleration time scale is given by Refs [5, 23].

$$t'_{acc} = \frac{\mathcal{E}'}{\eta c^2 Z e B'}$$

where Z is the number of unit charges such that $Z = 1$ for proton and $Z = 26$ for iron, $\mathcal{E}'$ is the energy of the accelerated particle, and η is the acceleration efficiency, which is set to be 1.

The synchrotron time scale $t'_{sync,p}$ is defined as

$$t'_{sync,p} = \frac{9\pi\epsilon_0 m_p^4 c^5}{|q|^4 B'^2 \mathcal{E}'}$$

where ϵ_0 is the permittivity of free space.

$\mathcal{E}'_{p,max}$ is the energy when $t'_{sync}/t'_{acc} = 1$. Therefore

$$\mathcal{E}'_{p,max} = \sqrt{\frac{9\pi\epsilon_0 m_p^4 c^7}{|e|^3 B'}} \ . \tag{3.8}$$

Likewise, we can determine the acceleration limit of iron too:

$$\mathcal{E}'_{Fe,max} = \sqrt{\frac{9\pi\epsilon_0 (56 m_p)^4 c^7}{(26|e|)^3 B'}} \simeq 23.7 \mathcal{E}'_{p,max} \ .$$

3.2.2 The neutrino spectrum from the pion source

Let us recall the photon-pion reaction:

$$p + \gamma \to \Delta^+ \to p + \pi^0 \ . \tag{3.9}$$

The enhanced reaction cross section at the Δ resonance is reflected by the energy break of photon $\mathcal{E}'_\gamma$ (in shock frame). The proton energy must satisfy the condition [13]

$$\mathcal{E}'_p \geq \frac{m_\Delta^2 c^4 - m_p^2 c^4}{4\mathcal{E}'_\gamma} \tag{3.10}$$

where m_Δ is the Δ mass. We can derive the break-energy in the observer's frame:

$$\mathcal{E}_{p,br} = \Gamma^2 \frac{m_\Delta^2 c^4 - m_p^2 c^4}{4\mathcal{E}_{\gamma,br}} \ . \tag{3.11}$$

In the photon-pion reaction pion takes about 20% of the proton energy and the muon-neutrino takes about 25% of the pion energy. The break energies of pion $\mathcal{E}_{\pi,br}$ and that of the muon neutrino $\mathcal{E}_{\nu_\mu,br}$ are

$$\mathcal{E}_{\pi,br} \approx 0.2\Gamma^2 \frac{m_\Delta^2 c^4 - m_p^2 c^4}{4\mathcal{E}_{\gamma,br}} \tag{3.12}$$

and

$$\mathcal{E}_{\nu_\mu,br} \approx 0.05\Gamma^2 \frac{m_\Delta^2 c^4 - m_p^2 c^4}{4\mathcal{E}_{\gamma,br}} \tag{3.13}$$

respectively. Without considering the synchrotron effect and the existence of maximal proton energy, we have the following pion and muon neutrino energy spectrum

$$\mathcal{E}_\pi^2 \frac{dI_\pi}{d\mathcal{E}_\pi}(\mathcal{E}_\pi) \propto \begin{cases} \mathcal{E}_\pi^{\alpha_2} & \text{if } \mathcal{E}_\pi \le \mathcal{E}_{\pi,br} \\ \mathcal{E}_\pi^{\alpha_1} & \text{if } \mathcal{E}_\pi \ge \mathcal{E}_{\pi,br} \end{cases} \tag{3.14}$$

and

$$\mathcal{E}_{\nu_\mu}^2 \frac{dI_{\nu_\mu}}{d\mathcal{E}_{\nu_\mu}}(\mathcal{E}_{\nu_\mu}) \propto \begin{cases} \mathcal{E}_{\nu_\mu}^{\alpha_2} & \text{if } \mathcal{E}_{\nu_\mu} \le \mathcal{E}_{\nu_\mu,br} \\ \mathcal{E}_{\nu_\mu}^{\alpha_1} & \text{if } \mathcal{E}_{\nu_\mu} \ge \mathcal{E}_{\nu_\mu,br} \end{cases} . \tag{3.15}$$

These break energies are related to Γ and B' as given by Eq.(3.5).

We note that the synchrotron loss effect of the pion should be considered as well. The characteristic synchrotron loss energy is derived by equating the decay time scale $t'_{decay,\pi}$ to the synchrotron loss time scale $t'_{sync,\pi}$ of charged pion. Since $t'_{sync,\pi} = \frac{9\pi\epsilon_0 m_\pi^4 c^5}{e^4 B'^2 \mathcal{E}'_\pi}$ and $t'_{decay,\pi} = \frac{\mathcal{E}'_\pi \tau_{0,\pi}}{m_\pi c^2}$, we have

$$\mathcal{E}_{\pi,sync} = \sqrt{\frac{9\pi\epsilon_0 m_\pi^5 c^7}{B'^2 e^4 \tau_{0,\pi}}} \tag{3.16}$$

where $\tau_{0,\pi} \approx 2.6 \times 10^{-8}$ is the life time of charged pion at rest.
The neutrino energy corresponding to $\mathcal{E}_{\pi,sync}$ is then given by

$$\mathcal{E}_{\nu_\mu,sync} = 0.25\sqrt{\frac{9\pi\epsilon_0 m_\pi^5 c^7}{B'^2 e^4 \tau_{0,\pi}}} . \tag{3.17}$$

With synchrotron loss effect taken into account, we arrive at the following expectation

$$\mathcal{E}_{\nu_\mu}^2 \frac{dI_{\nu_\mu}}{d\mathcal{E}_{\nu_\mu}}(\mathcal{E}_{\nu_\mu}) \propto \begin{cases} \mathcal{E}_{\nu_\mu}^{\alpha_2} & \text{if } \mathcal{E}_{\nu_\mu} \leq \mathcal{E}_{\nu_\mu,br} \\ \mathcal{E}_{\nu_\mu}^{\alpha_1} & \text{if } \mathcal{E}_{\nu_\mu,br} \leq \mathcal{E}_{\nu_\mu} \leq \mathcal{E}_{\nu_\mu,sync} \\ \mathcal{E}_{\nu_\mu}^{\alpha_1}\mathcal{E}_{\nu_\mu}^{-2} & \text{if } \mathcal{E}_{\nu_\mu} \geq \mathcal{E}_{\nu_\mu,sync} \end{cases} . \tag{3.18}$$

To derive the neutrino spectrum more realistically, we follow the treatment in Ref. [19] while imposing the maximal proton energy (which does not appear in [19]). We consider the pion spectrum before taking the synchrotron effect on pions and with a maximal pion energy (from the proton maximal energy imposed). ϕ_π behaves as

$$\phi_\pi(\mathcal{E}_\pi) \propto \begin{cases} \mathcal{E}_\pi^{\alpha_2}\mathcal{E}_\pi^{-2} & \text{if } \mathcal{E}_\pi \leq \mathcal{E}_{\pi,br} \\ \mathcal{E}_\pi^{\alpha_1}\mathcal{E}_\pi^{-2} & \text{if } \mathcal{E}_{\pi,br} \leq \mathcal{E}_\pi \leq \mathcal{E}_{\pi,max} \\ \exp(-\frac{\mathcal{E}_\pi}{\mathcal{E}_{\pi,max}}) & \text{if } \mathcal{E}_\pi \geq \mathcal{E}_{\pi,max} \end{cases} . \tag{3.19}$$

Here $\mathcal{E}_{\pi,br}$ is given by Eq. (3.12) and $\mathcal{E}_{\pi,max}$ can be derived by Eq. (3.8), i.e.,

$$\mathcal{E}_{\pi,max} \approx 0.05\Gamma\sqrt{\frac{9\pi\epsilon_0 m_p^4 c^7}{|e|^3 B'}} . \tag{3.20}$$

After taking the synchrotron effect, the final muon neutrino spectrum should be

$$\frac{dI_{\nu_\mu}}{d\mathcal{E}_{\nu_\mu}}(\mathcal{E}_{\nu_\mu}) = -\frac{\partial}{\partial\mathcal{E}_{\nu_\mu}} \int_{4\mathcal{E}_{\nu_\mu}}^{\infty} d\mathcal{E}_i \phi_\pi(\mathcal{E}_i) P_\pi(\mathcal{E}_i, 4\mathcal{E}_{\nu_\mu}) \tag{3.21}$$

where $\phi_\pi(\mathcal{E}_i)$ is flux of pions produced at the source with energy $\mathcal{E}_i$. $P_\pi(\mathcal{E}_i, \mathcal{E}_f)$ is the decaying probability of a particle which is losing energy from the initial energy $\mathcal{E}_i$ to the final energy $\mathcal{E}_f$.

$$P(\mathcal{E}_i, \mathcal{E}_f) = 1 - \exp\left(-\mathcal{E}_{\pi,sync}^2 \frac{(\mathcal{E}_f^{(-2)} - \mathcal{E}_i^{(-2)})}{2}\right) . \tag{3.22}$$

This probability is obtained for particles which lose energy by the synchrotron effect (see the appendix, taking $n = 2$).

We calculate Eq.(3.21) numerically to obtain the spectrum of muon neutrinos arising from pion decays.

3.2.3 The neutron beam spectrum

The spectrum of anti-electron neutrino from the neutron β-decay is similar to the pion spectrum. However the neutron is not affected by the magnetic field, so that the anti-electron neutrino spectrum is only constrained by the break energy and the maximal energy:

$$\phi_{\nu_e} = \frac{dI_{\nu_e}}{d\mathcal{E}_{\nu_e}} \propto \begin{cases} \mathcal{E}_{\nu_e}^{\alpha_2}\mathcal{E}_{\nu_e}^{-2} & \text{if } \mathcal{E}_{\nu_e} \leq \mathcal{E}_{\nu_e,br} \\ \mathcal{E}_{\nu_e}^{\alpha_1}\mathcal{E}_{\nu_e}^{-2} & \text{if } \mathcal{E}_{\nu_e,br} \leq \mathcal{E}_{\nu_e} \leq \mathcal{E}_{\nu_e,max} \\ \exp(-\frac{\mathcal{E}_{\nu_e}}{\mathcal{E}_{\nu_e,max}}) & \text{if } \mathcal{E}_{\nu_e} \geq \mathcal{E}_{\nu_e,max} \end{cases} . \tag{3.23}$$

In the photon-pion reactions the neutron takes about 80% of the proton energy. The anti-electron neutrino takes about 0.1% of the neutron energy in the β-decay. The break energies of anti-electron neutrino $\mathcal{E}_{\nu_e,br}$ and $\mathcal{E}_{\nu_e,max}$ (from Eq. (3.8)) are given by

$$\mathcal{E}_{\nu_e,br} \approx 0.0008\mathcal{E}_{p,br} = 0.0008\Gamma^2\frac{m_\Delta^2c^4 - m_p^2c^4}{4\mathcal{E}_\gamma} , \tag{3.24}$$

and

$$\mathcal{E}_{\nu_e,max} \approx 0.0008\mathcal{E}_{p,max} = 0.0008\Gamma\sqrt{\frac{9\pi\epsilon_0 m_p^4c^7}{|e|^3B'}} . \tag{3.25}$$

3.2.4 The normalization

To get the expected neutrino intensity on Earth, we refer to the fluence F_γ measured by the BATSE data. We choose the average $F_\gamma = 10^{-5}$ erg/cm^2.

The normalization factor F_{ν_μ} of muon-neutrino from pion decay is given by Ref. [13].

$$F_{\nu_\mu} \approx \frac{1}{8}\frac{1}{\xi_e}0.2F_\gamma\frac{L_{\gamma,52}}{\Gamma_{2.5}^4 t_{v,-2}(\mathcal{E}_{\gamma,br}/\text{MeV})} \tag{3.26}$$

where $\Gamma_{2.5} = \Gamma/10^{2.5}$, $L_{\gamma,52} = L_\gamma/(10^{52}\text{erg/s})$, and $t_{v,-2} = t_v/(0.01\text{s})$.

The anti-electron neutrino from the neutron β-decay takes a less energy fraction (0.0008) of proton comparing to the fraction (0.05) of the muon neutrino taken by (from pion decay). The normalization in neutron beam should be less by the factor $(0.05/0.0008)^{-2}$. Hence $F_{\nu_e} \approx (0.05/0.0008)^{-2} \times F_{\nu_\mu}$. This is caused by different shifting factors from the proton spectrum, as illustrated by Fig. 3.2. We note that the exponent -2 is from the proton spectrum.

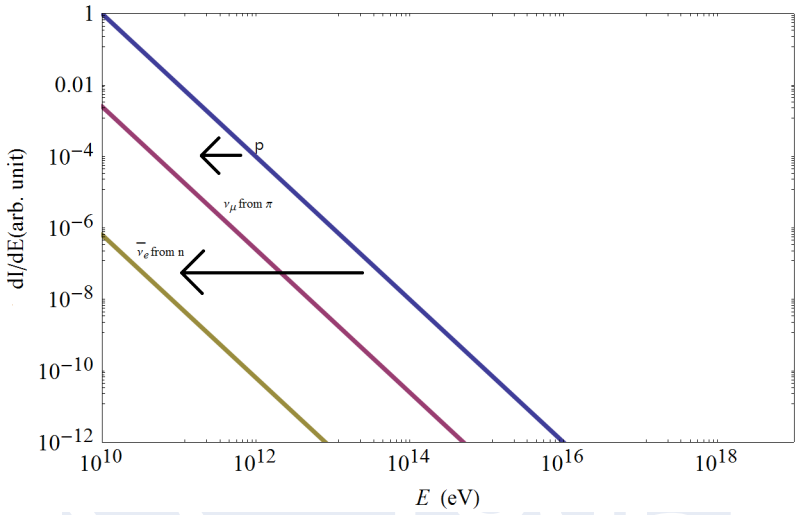

Figure 3.2: The sketch of spectrum shifting

The normalization factors F_{ν_μ} and F_{ν_e} are for single GRB. Taking the expected 300 GRBs a year (365×86400 seconds) in the full sky survey (4π solid angle), the expected flux is $F \times 300/365/86400/4\pi \times \phi$ (unit energy per unit area per second per solid angle). Here $F = F_{\nu_\nu}, F_{\nu_e}$ and $\phi = \phi_{\nu_\nu}, \phi_{\nu_e}$ respectively.

To determine the dominating source, we have to compare the integrated

flux in the observable energy region. The integrated flux is given by

$$I_\nu = \int_{\mathcal{E}_{\rm ex,min}}^{\mathcal{E}_{\rm ex,max}} \frac{dI_\nu}{d\mathcal{E}_\nu} d\mathcal{E}_\nu \ . \tag{3.27}$$

Here we choose the region $\mathcal{E}_{\rm ex,min} = 10^{11}$eV and $\mathcal{E}_{\rm ex,max} = 10^{15}$eV such as the IceCube experiment region. The synchrotron effects on muon is neglected. In this condition we can regard the ν_μ from π as the pure pion beam source ($\phi_{\nu_e} : \phi_{\nu_\mu} : \phi_{\nu_\tau} = 1 : 2 : 0$) and $\bar{\nu_e}$ from n as the pure neutron beam source ($\phi_{\nu_e} : \phi_{\nu_\mu} : \phi_{\nu_\tau} = 1 : 0 : 0$). The result is the composition of the two. We present the ratio I_{ν_e}/I_{ν_μ} in this region.

3.3 Our settings and results

We assume pure protons (with no heavy nuclei) to be accelerated in the source.

Eq.(3.2) can be written as

$$\frac{8\pi c^3 t_v^2 \Gamma^6 B'^2}{\mu_0} = \frac{\xi_B L_\gamma}{\xi_e} \ ,$$

which can be recasted as the condition $f(B', \Gamma, t_v, L_\gamma) =$ constant. Note that $r_i = 2\Gamma^2 c t_v$, by Eq.(3.1). t_v is a fixed parameter in our calculation. A common choice [13, 28] which we do not use is to take L_γ and Γ as independent variables, and treat B' as a response variable. However, we are interested in magnetic effects on $\mathcal{E}_{\pi,sync}$ and $\mathcal{E}_{\nu_e,max}$. In that case we vary B' and Γ independently, and therefore the photon luminosity L_γ is the response variable. The neutrino flux spectra depend on the measured photon spectrum slope indices α_1 and α_2 as shown in Eq. (3.3). $\alpha_1 \approx 0$ is fixed while α_2 is a variable.

First of all, we summarize the physical range of each parameter here.

Limits on measurement

The most typical measured $\mathcal{E}_{\gamma,br}$ from GRB is in the range

$$0.1 \text{ MeV} \lesssim \mathcal{E}_{\gamma,\text{br}} \lesssim 0.3 \text{ MeV} .$$

The full range of $\mathcal{E}_{\gamma,br}$ is

$$10 \text{ keV} \lesssim \mathcal{E}_{\gamma,\text{br}} \lesssim 100 \text{ MeV} .$$

The ranges for photon spectra indices are

$$\alpha_1 \lesssim 0, \text{ and } \quad \alpha_2 \lesssim 4,$$

In most of all GRBs, we have $\alpha_2 = 1.0 - 1.2$.
The range for GRB luminosity is

$$10^{50-51} \text{ erg/s} \lesssim L_\gamma \lesssim 10^{53-54} \text{ erg/s} .$$

Here the lower limit can be less for X-ray candidates , i.e., bursts with photon energy in the X-ray region. L_γ is determined from other measurement and models, like the afterglow observation. It is model dependent. It is hard to say whether L_γ is a measurement or a model parameter.

Model parameters Γ and B'

Typical values of these parameters at GRBs are

$$\Gamma \approx 300 ,$$

$$B' \approx (3 - 30) \text{ Tesla} ,$$

which correspond to

$$L_\gamma \sim (10^{51} - 10^{53}) \text{ erg/s} .$$

The full ranges of GRB model parameters are

$$100 \lesssim \Gamma \lesssim 1000$$

and

$$0.1 \text{ Tesla} \lesssim B' \lesssim 10^3 \text{ Tesla} .$$

Fixed parameters

The variability time is held fixed, i.e.,

$$t_v = 10 \text{ ms} .$$

The energy fractions taken by electrons and magnetic field from the total GRB luminosity are

$$\xi_e = \xi_B = 0.3 .$$

The photon spectrum index (before break) is

$$\alpha_1 \approx 0 .$$

3.3.1 The neutrino spectra given by different Γ and B'

We survey the full magnetic field range $B' = 0.1 - 1000$ Tesla for $\Gamma = 100$ (lower limit), $\Gamma = 300$ (typical value) and $\Gamma = 1000$ (upper limit). Note that $L_\gamma \propto \Gamma^6 B'^2$. A higher B' implies a lower Γ to make L_γ not exceeding the limit of L_γ. The spectrum index $\alpha_2 = 1.2$ is also held fixed here.

The resulting neutrino spectra are given in Fig. 3.4, 3.5 and 3.6, The expected measurements are given by Table 3.1.

3.3.2 The neutrino spectra resulting from different α_2 indices

Here we fixed $\Gamma = 300$ and $B' = 10$ Tesla for a typical GRB. The spectrum index $\alpha_2 = 1.0,\ 1.2,\ 2.0,\ 3.0$ is the only variable here. The resulting spectra are given by Fig. 3.8, 3.9, 3.10, and 3.11. Expected measurements are given by Table 3.2.

3.4 Discussion and summary

The existence of pure neutron beam

Moharana and Gupta [28] suggest a pure neutron beam source dominating for $\mathcal{E}_\nu > 10^{18}$ eV. The calculation is based on a synchrotron loss effect caused by the magnetic field on charged pion π^+. On the contrary the uncharged neutron n is not affected by the magnetic field. Their result is shown in Fig. 3.3.

Our result

The synchrotron effect

Our results as shown in Fig. 3.4, which do not agree those in Ref. [28]. Our result does not confirm the existence of a pure neutron source at higher energy range for typical GRB parameters. Note that the green curves in Fig. 3.4 correspond to the pair of curves with ($L = 10^{52}$erg/s) in Fig. 3.3.

It is possible to find a pure neutron beam from GRB with extremely high magnetic field. However, this result is arguable on two points. The first one is the choice of the proton spectrum cut-off. The neutrino fluxes resulting

from different choices of proton spectrum cut-off are shown in Fig. 3.7. Our cut-off choice allows a dominant neutron beam source at high energy while the cut-off choice made by Ref. [23] does not allow this dominance. At this moment we do not know the behaviour of proton flux beyond $\mathcal{E}_{p,max}$. The other point is that the flux with high magnetic field strength may exceed the cosmic ray limit. This implies that the neutron beam source is very rare even if it truly exists. Furthermore, a neutron beam source with such a high energy ($\gtrsim 10^{17}$eV) may be mixed with a pion beam from GZK neutrino. Therefore it is not possible to isolate the neutron beam source ($\gtrsim 10^{17}$eV) from observations.

Dependence on the photon spectrum index

We do not find pure neutron beam for typical choices $\alpha_2 = 1.0 - 1.2$. On the other hand, for GRBs with steeper spectra $\alpha_2 \geq 2$, there may be a pure neutron beam in the lower energy region, as shown in Fig. 3.10 and 3.11. For $\alpha_2 \gtrsim 3$ we obtain a pure neutron beam in the IceCube energy region $(10^{11} - 10^{15})$eV for some special GRBs. GZK pion beam does not affect this low-energy region.

The expected neutrino flux on Earth

For the $(10^{11} - 10^{15})$eV energy region, we find that for typical GRB, $I_{\nu_e}/I_{\nu_\mu} \approx 0.63$, as shown in Table 3.1, *i.e.*, $\phi_{\nu_e} : \phi_{\nu_\mu} : \phi_{\nu_\tau} \approx 1 : 1.59 : 0$ (without oscillation) in the region $(10^{11} - 10^{15})$eV. We then suggest a mixed beam instead of a pure-pion beam for typical GRB. Table 3.1 show the tendency that for GRBs with larger B', one may obtain a smaller I_{ν_e}/I_{ν_μ} ratio in the energy region $(10^{11} - 10^{15})$eV. Table 3.2 shows the tendency that larger α_2 produces a larger I_{ν_e}/I_{ν_μ} ratio.

$\Gamma = 100$, $\alpha_2 = 1.2$					
B' (Tesla)	$\mathcal{E}_{\gamma,br}$ (MeV)	L_γ (10^{52}erg/s)	I of π beam (1:2:0) $\mathrm{cm^{-2}s^{-1}sr^{-1}}$	I of n beam (1:0:0) $\mathrm{cm^{-2}s^{-1}sr^{-1}}$	I_{ν_e}/I_{ν_μ}
1000	3.5	13.54	1.01×10^{-11}	8.08×10^{-13}	0.54
300	1.05	1.21	9.80×10^{-13}	1.00×10^{-13}	0.55
100	0.35	0.14	1.11×10^{-13}	1.33×10^{-14}	0.56
Typical GRBs, $\Gamma = 300$, $\alpha_2 = 1.2$					
B' (Tesla)	$\mathcal{E}_{\gamma,br}$ (MeV)	L_γ (10^{52}erg/s)	I of π beam (1:2:0) $\mathrm{cm^{-2}s^{-1}sr^{-1}}$	I of n beam (1:0:0) $\mathrm{cm^{-2}s^{-1}sr^{-1}}$	I_{ν_e}/I_{ν_μ}
30	0.32	8.89	7.49×10^{-15}	1.49×10^{-15}	0.60
10	0.11	0.99	6.68×10^{-16}	1.75×10^{-16}	0.63
3	0.032	0.089	4.72×10^{-17}	1.57×10^{-17}	0.67
$\Gamma = 1000$, $\alpha_2 = 1.2$					
B' (Tesla)	$\mathcal{E}_{\gamma,br}$ (MeV)	L_γ (10^{52}erg/s)	I of π beam (1:2:0) $\mathrm{cm^{-2}s^{-1}sr^{-1}}$	I of n beam (1:0:0) $\mathrm{cm^{-2}s^{-1}sr^{-1}}$	I_{ν_e}/I_{ν_μ}
1	0.035	13.54	3.31×10^{-18}	1.21×10^{-18}	0.68
0.3	0.011	1.21	2.34×10^{-19}	8.57×10^{-20}	0.68
0.1	0.0035	0.14	2.09×10^{-20}	7.64×10^{-21}	0.68

Table 3.1: The expected neutrino integrated flux (right from the vertical line) on Earth, for $\Gamma = 100, 300, 1000$. The neutrino oscillation is not taken into account here.

$\Gamma = 300$, $B' = 10$Tesla			
α_2	I of π beam (1:2:0) $\mathrm{cm^{-2}s^{-1}sr^{-1}}$	I of n beam (1:0:0) $\mathrm{cm^{-2}s^{-1}sr^{-1}}$	I_{ν_e}/I_{ν_μ}
1.0	2.16×10^{-15}	2.96×10^{-16}	0.57
1.2	6.68×10^{-16}	1.75×10^{-16}	0.63
2.0	3.34×10^{-17}	7.07×10^{-17}	1.56
3.0	2.39×10^{-18}	5.20×10^{-17}	11.38

Table 3.2: The expected neutrino integrated flux on Earth. The neutrino oscillation is not taken into account here.

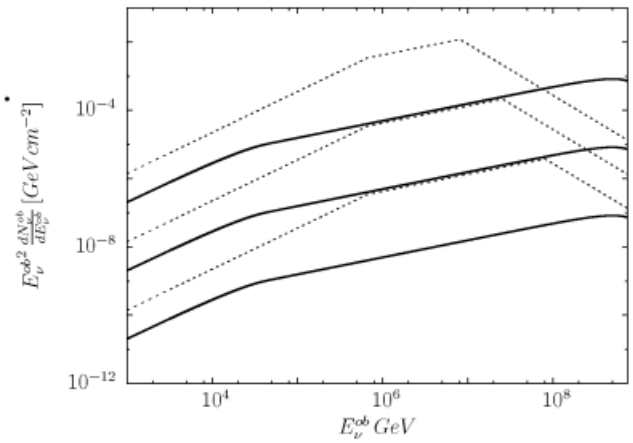

Figure 3.3: Neutrino flux from pion decay (dashed line) and neutron β-decay (solid line) in GRB with $L = 10^{52}$, 10^{51}, 10^{50} erg/s, $\Gamma = 300$, $t_v = 10$ms. (Moharana and Gupta 2010) [28]

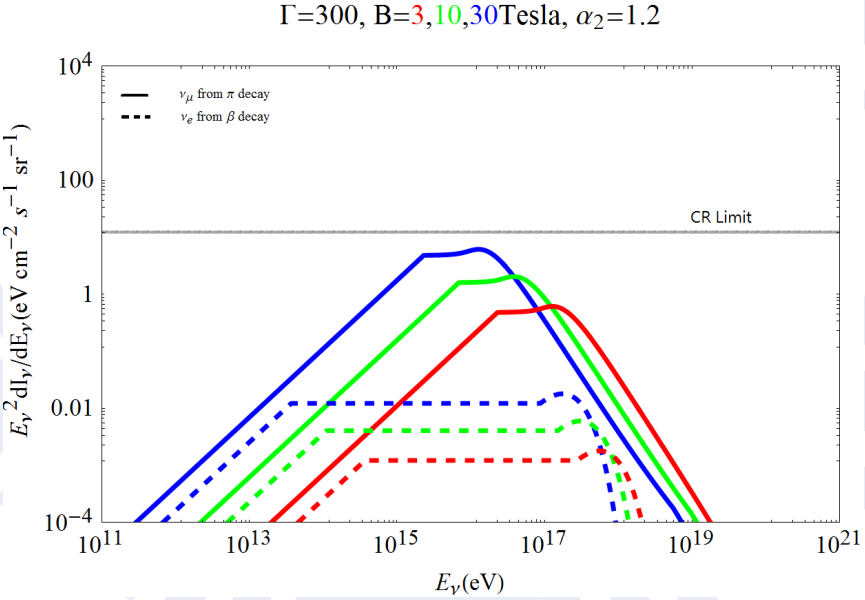

Figure 3.4: Typical GRB neutrino spectra, with $\Gamma = 300$, B'=3(red), 10(green), 30(blue) Tesla. The solid line is ν_μ flux from pion decays ((1:2:0) source), and the dashed line is $\bar{\nu}_e$ flux from neutron β-decays ((1:0:0) source).

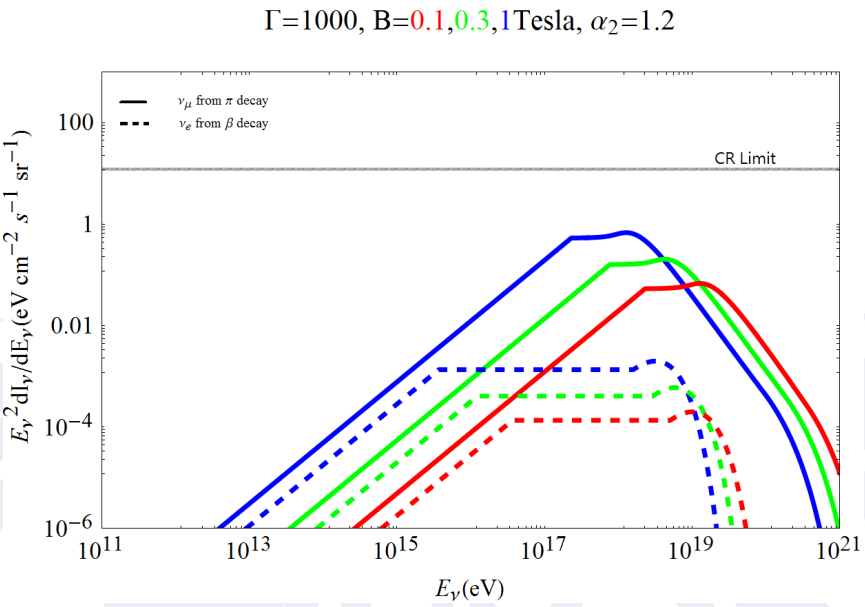

Figure 3.5: Γ = 1000, B'=0.1(red), 0.3(green), 1.0(blue)Tesla. The solid line is ν_μ flux from pion decays ((1:2:0) source), and the dashed line is $\bar{\nu}_e$ flux from neutron β-decays ((1:0:0) source).

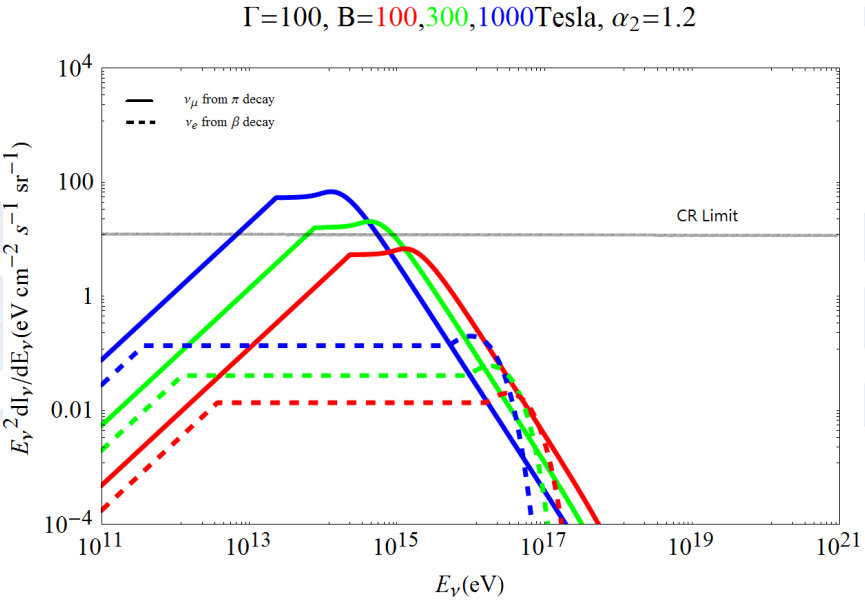

Figure 3.6: Γ = 100, B'=100(red), 300(green), 100(blue) Tesla. The solid line is ν_μ flux from pion decays ((1:2:0) source), and the dashed line is $\bar{\nu}_e$ flux from neutron β-decays ((1:0:0) source).

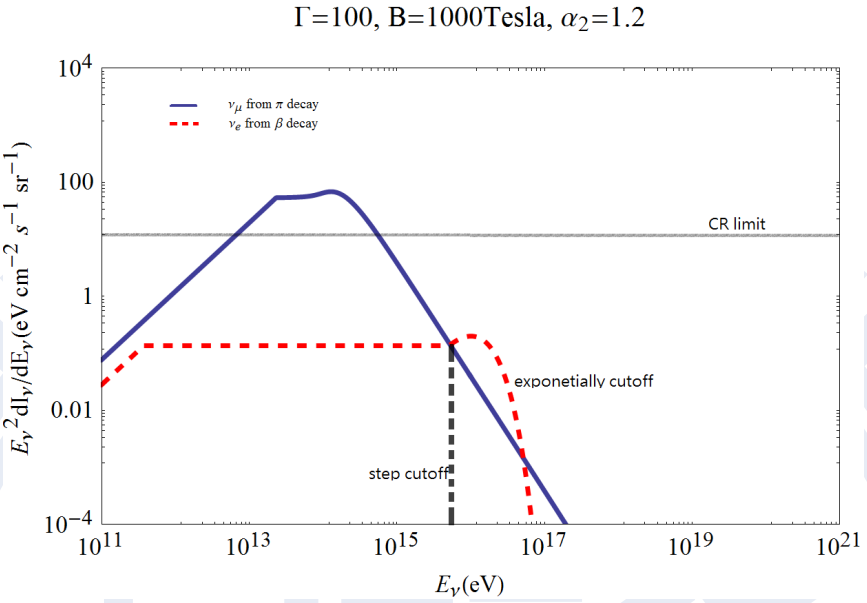

Figure 3.7: The vertical (black-dashed) line results from the cut-off suggested by Hümmer *et al.* [23] as given by Eq. (3.6). The red-dashed line results from the cut-off we choose as given by Eq. (3.7).

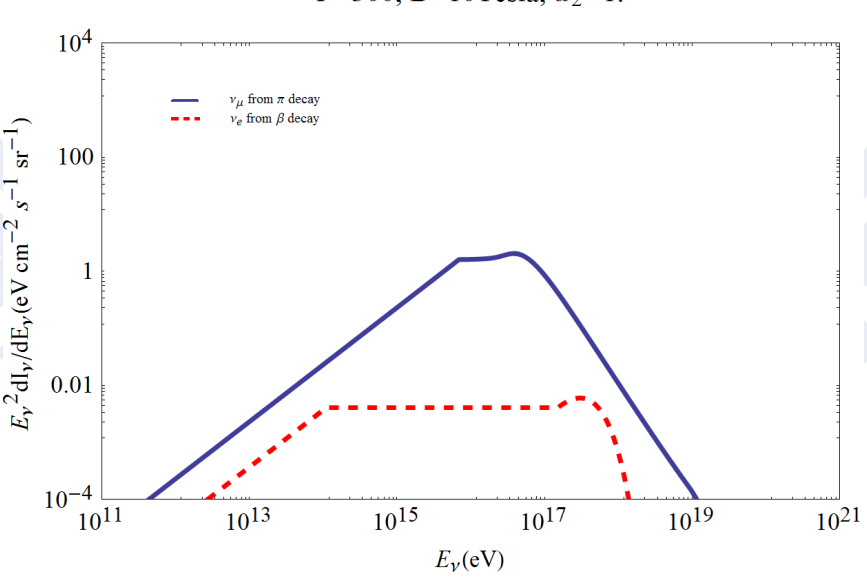

Figure 3.8: $\Gamma = 300$, B'= 10 Tesla, $\alpha_2 = 1.0$

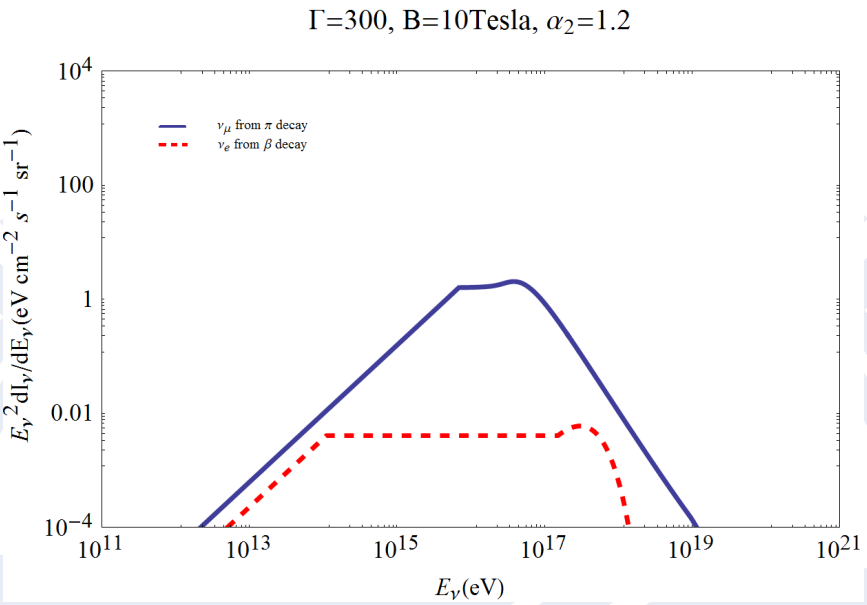

Figure 3.9: $\Gamma = 300$, B'= 10 Tesla, $\alpha_2 = 1.2$

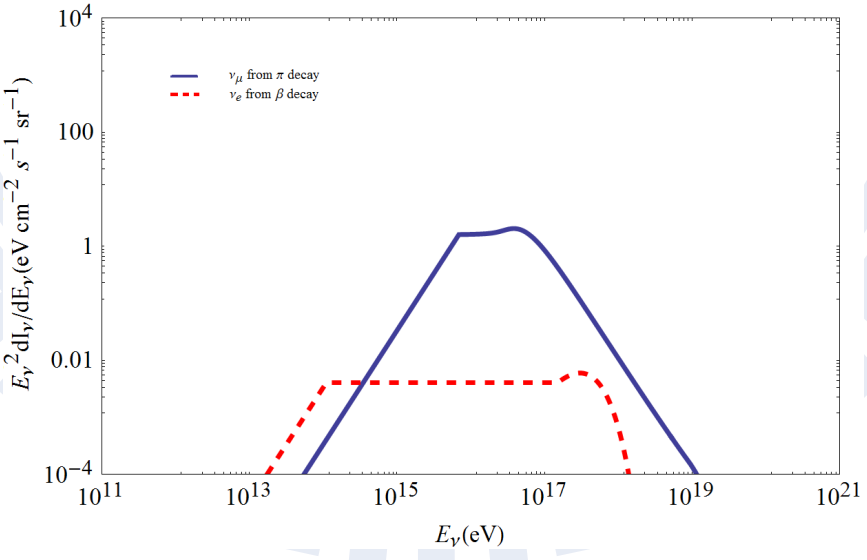

Figure 3.10: $\Gamma = 300$, B'= 10 Tesla, $\alpha_2 = 2.0$

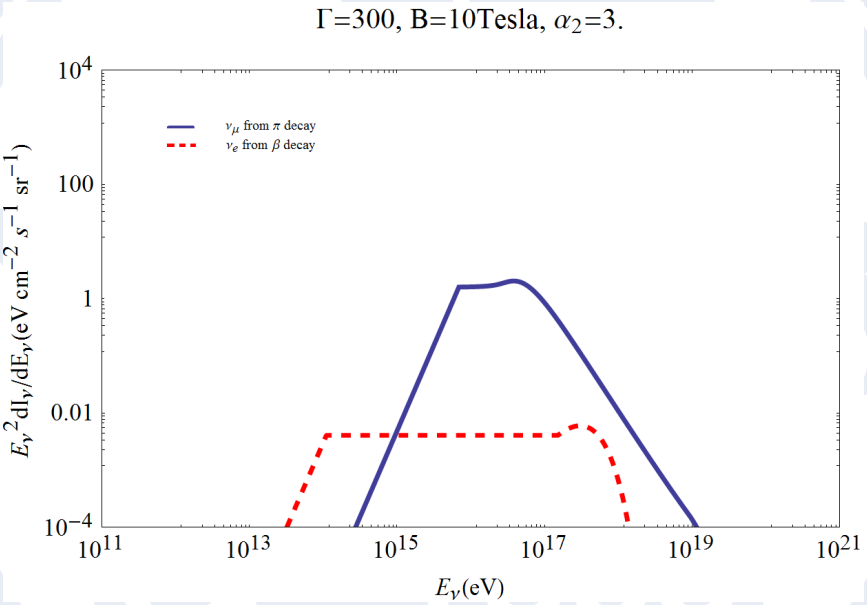

Figure 3.11: $\Gamma = 300$, B'= 10 Tesla, $\alpha_2 = 3.0$

Chapter 4

Conclusion

To study the properties of the UHECR sources, the neutrino flux and its flavor composition are the keys. The neutrino flavor composition has been regarded as a pure pion beam. The neutrino from neutron β-decay has been neglected before.

We take gammay-ray bursts as the leading candidate of UHECR. We predict the GRB neutriono flux before oscillation. Moharana and Gupta argued that there exists a pure neutron beam (before oscillation) in the high energy range ($\mathcal{E}_\nu > 10^{18}$ eV) for a typical GRB. This result is inconsistent in our view.

Our calculation focus on the magnetic field effects on energy losses of protons and pions. The other parameter considered is the photon spectrum index α_2. We choose $z = 0$, take the source as pure proton, and neglect the muon energy loss. Our result does not take into account neutrino oscillations. The experimentally measured mixing parameters can be applied to calculate expected neutrino flavor ratio on Earth.

In summary, we predict the neutrino fluxes for typical GRBs. We also calculated neutrino fluxes the GRBs with larger magnetic field strength and

the GRBs with different photon spectra indices.

We present the expected flux in the full energy range $(10^{11} - 10^{21})$ eV. For an experimental consideration, the flux is also integrated in the IceCube energy range$(10^{11} - 10^{15})$ eV.

For a typical GRB the prediction for neutrino flavor composition is given as follows. The neutrino flavor composition behaves as that from a mixed source $\phi_{\nu_e} : \phi_{\nu_\mu} : \phi_{\nu_\tau} \approx 1 : 1.5 : 0$ in the low energy region, and behaves as that from a pure pion beam in the higher energy range $\phi_{\nu_e} : \phi_{\nu_\mu} : \phi_{\nu_\tau} \approx 1 : 2 : 0$. The pure neutron beam does not generally occur for relatively high energy. Even for extremely high magnetic field, the chance for a pure neutron beam is quite small.

For large photon spectra indices, such a pure neutron beam source may exist in the lower energy region. This certainly depends on the fitting of the photon spectrum.

We conclude that the pure neutron beam do not occur for typical GRBs. The pure neutron beam is still not likely to occur in the higher energy range in GRBs with extremely high magnetic field. The existence of pure neutron beam in IceCube energy range $(10^{11} - 10^{15})$ eV is possible, depending on the photon indices.

Appendix A

Details of derivations

A.1 The energy loss time

Consider: a moving particle with velocity $\vec{u}$ in S, $\vec{u}'$ in S'

S: the lab frame,

S': the rest frame of the moving particle,

$\vec{v} \parallel \vec{x}$: the relative velocity between two coordinates.

a_x can be derived by the inverse Lorentz transformation:

$$u_x = \frac{u'_x + v}{1 + \frac{v}{c^2}u'_x} .$$

$$t = \Gamma(t' + \frac{v}{c^2}x') .$$

$$du_x = \frac{du'_x}{\Gamma^2(1 + \frac{v}{c^2}u'_x)^2} .$$

$$dt = \Gamma dt'(1 + \frac{v}{c^2}\frac{dx'}{dt'}) = \Gamma dt'(1 + \frac{v}{c^2}u'_x) .$$

$$a_x = \frac{du_x}{dt} = \frac{1}{\Gamma^3(1 + \frac{v}{c^2}u'_x)^3}a'_x .$$

Likewise, we can get a_y by same process:

$$a_y = \frac{a'_y}{\Gamma^2(1+\frac{v}{c^2}u'_x)^2} - \frac{u'_y v}{c^2}\frac{a'_x}{\Gamma^2(1+\frac{v}{c^2}u'_x)^3} \ .$$

WLOG, choosing $u_\parallel \parallel \vec{x}$, and $u_\perp \parallel \vec{y}$.

S' is the rest frame of the particle, i.e., $u'_x = u'_y = 0$

Consequently,

$$a_\parallel = a_x = \frac{a'_\parallel}{\Gamma^3}$$

and

$$a_\perp = a_y = \frac{a'_\perp}{\Gamma^2} \ .$$

Consider the particle to be charged with q, moving ultra-relativistically in a uniform magnetic field $\vec{B}$, and hence it will radiate.

The radiation power is referred to the Larmor formula [Landau]:

$$I = -\frac{d\mathcal{E}}{dt} = \frac{2q^2|a'|^2}{3c^3} = \frac{2q^2}{3c^3}({a'_\perp}^2 + {a'_\parallel}^2) = \frac{2q^2}{3c^3}(\Gamma^4 a_\perp^2 + \Gamma^6 a_\parallel^2) \ . \qquad \text{(A.1)}$$

Substituting $a_\parallel = 0$ and $a_\perp = \frac{quB}{mc\Gamma}$ into (A.1), we can obtain

$$-\frac{d\mathcal{E}}{dt} = \frac{2q^2}{3c^3}\Gamma^2\frac{q^2B^2}{m^2c^2}u_\perp^2 \ .$$

$$-\frac{d\mathcal{E}}{dt} = \frac{2}{3}\frac{q^4}{m^2c^4}c\Gamma^2B^2\beta_\perp^2 \ .$$

Consider a spherical homogeneous velocity.

The mean square velocity can be derived by averaging over an isotropic distribution of pitch angles α :

$$< \beta_\perp^2 >= \frac{\beta^2}{4\pi}\int \sin^2\alpha d\Omega$$

where the pitch angle is the angle between the magnetic field and the particle moving direction.

Here we consider uniform $\vec{B} \parallel \vec{z}$, and then $\alpha = \theta$.

$$\int_{\theta=0}^{\theta=\pi}\int_{\phi=0}^{\phi=2\pi} \sin^2\alpha d\Omega = \int_{\theta=0}^{\theta=\pi}\int_{\phi=0}^{\phi=2\pi} \sin^2\theta \sin\theta d\theta d\phi = \frac{8\pi}{3} ,$$

$$< \beta_\perp^2 >= \frac{2}{3}\beta^2 .$$

$$-\frac{d\mathcal{E}}{dt} = \frac{4q^2}{9c^3}\Gamma^2\frac{q^2B^2}{m^2c^2}u^2 = \frac{4q^4B^2\mathcal{E}^2}{9m^4c^7} \equiv A\mathcal{E}^2 .$$

Synchrotron loss time, defined as

$$t \equiv (A\mathcal{E})^{(-1)} ,$$

will be exact as the time it takes the particle to lose **half** of its energy due to synchrotron losses in a constant magnetic field.

$$t_{sync} = \frac{9m^4c^7}{4q^4B^2\mathcal{E}_0} \tag{A.2}$$

where m is the rest mass of the particle, $\mathcal{E}_0$ is the initial total energy.

Here we introduce an equivalent common expression of (A.2):

$$t_{sync} = \frac{3m^4c^3}{4\sigma_T m_e^2 \mathcal{E}_0 U_B}$$

where σ_T is the Thomson total cross section, U_B is the magnetic field energy density.

$$\sigma_T = \frac{8}{3}\pi\left(\frac{q^2}{m_ec^2}\right)^2 .$$

$$U_B = \frac{B^2}{8\pi} .$$

The above mentioned formulae are in Gaussian units; furthermore, we can represent t_{sync} in SI units:

$$t_{sync} = \frac{9\pi\epsilon_0 m^4 c^5}{q^4 B^2 \mathcal{E}_0}$$

by the transformation:

$$q \to \frac{1}{\sqrt{4\pi\epsilon_0}} q$$

and

$$B \to \sqrt{\frac{4\pi}{\mu_0}} B \ .$$

A.2 The decaying probability

Consider N_i particles with $\mathcal{E}_i$ initial energy, with decay time τ_i.

The Energy loss by time is

$$\frac{d\mathcal{E}}{dt} = -A\mathcal{E}^n \ . \tag{A.3}$$

The decay time, a function of Energy, can be written as

$$\tau = \tau_i(\mathcal{E}/\mathcal{E}_0)$$

where $\mathcal{E}_0$ is not the rest energy, but an enegy we choose to set loss time scale equals to the initial decay time.

$$t_{loss}^{-1}(\mathcal{E}) \equiv A\mathcal{E}^{(n-1)} \ .$$

$$t_{loss}^{-1}(\mathcal{E}_0) = \tau_i^{(-1)} = A\mathcal{E}_0^{(n-1)} \ . \tag{A.4}$$

Start from an exponential decaying function:

$$\frac{dN}{dt} = -\frac{1}{\tau}N \ .$$

$$\int_{N_i}^{N_f} \frac{dN}{N} = -\int_0^{t_f} \frac{1}{\tau} dt \ .$$

$$\int_{N_i}^{N_f} \frac{dN}{N} = -\int_{\mathcal{E}_i}^{\mathcal{E}_f} \frac{1}{\tau}\frac{dt}{d\mathcal{E}} d\mathcal{E} \ .$$

$$\log\left(\frac{N_f}{N_i}\right) = \int_{\mathcal{E}_i}^{\mathcal{E}_f} \frac{\mathcal{E}_0}{\tau_i}\frac{1}{A}\mathcal{E}^{-n-1} d\mathcal{E} \ .$$

Take exponet both LHS and RHS,

$$Q \equiv \frac{N_f}{N_i} = \exp\left(-\frac{\mathcal{E}_0}{\tau_i}\frac{1}{A}\frac{(\mathcal{E}_f^{(-n)} - \mathcal{E}_i^{(-n)})}{n}\right) \ .$$

$$Q = \exp\left(-\mathcal{E}_0^n \frac{(\mathcal{E}_f^{(-n)} - \mathcal{E}_i^{(-n)})}{n}\right) \ .$$

Here we erase τ_i and A by substituting (A.4)

Q is the fraction of living particles, so the decay probability is

$$P = 1 - Q = 1 - \exp\left(-\mathcal{E}_0^{(n)} \frac{(\mathcal{E}_f^{(-n)} - \mathcal{E}_i^{(-n)})}{n}\right) \ .$$

Appendix B

Table of symbols

Physical constants

Symbol	Definition	Numerical value	Unit
c	speed of light	299792458	m/s
ϵ_0	permittivity	8.85×10^{-12}	Farad/s
μ_0	permeability of vacuum	1.26×10^{-6}	H/m
e	(Abs.)electron charge	1.60×10^{-19}	C
m_e	electron mass	9.11×10^{-31}	kg
m_p	proton mass	1.67×10^{-27}	kg
m_Δ	delta mass	2.20×10^{-27}	kg
m_π	(charged) pion mass	2.49×10^{-28}	kg
$\hbar$	reduced Planck constant	1.05×10^{-34}	J s
$\tau_{0,\pi}$	(charged) pion life time	2.60×10^{-8}	s

Table B.1: Definitions and numerical values of constants

Parameters

Symbol	Description	Typical value	Unit
L_γ	photon luminosity of GRB	$10^{51} - 10^{53}$	erg/s
t_v	variability time of GRB	0.01	s
B'	magnetic field, in shock frame	10-30	Tesla
Γ	Lorentz factor, shock frame to observer's frame	300	
$\mathcal{E}_{\gamma,br}$	"break" energy of measured photon	0.1-0.3	MeV
F_γ	measured GRB photon fluence	10^{-5}	erg/cm^2
α_1	photon spectrum index 1	0	
α_2	photon spectrum index 2	1.0-1.2	

Table B.2: Descriptions and typical values of parameters

Bibliography

[1] E. Fermi, Phys. Rev. **75**, 1169 (1949).

[2] K. Greisen, Phys. Rev. Lett. **16**, 748 (1966).

[3] G. T. Zatsepin and V. A. Kuz'min, J. Exp. Theor. Phys. Lett. **4**, 78 (1966).

[4] J. A. Peacock, Mon. Not. R. astr. Soc. **196**, 135 (1981).

[5] A. M. Hillas, Ann. Rev. Astron. Astrophys. **22**, 425 (1984).

[6] N. Hayashida *et al.*, Phys. Rev. Lett. **73**, 3491 (1994).

[7] M. Fukugita and A. Suzuki, Physics and astrophysics of neutrinos. Tokyo:Springer-Verlag (1994).

[8] E. Waxman and J. N. Bahcall, Phys. Rev. **D59**, 023002 (1999).

[9] P. Bhattacharjee and G. Sigl, Phys. Rept. **327**, 109 (2000).

[10] E. Waxman, Lect. Notes Phys. **576**, 122 (2001).

[11] See Page 1-8. B. Paczynski(author), in the book: M. Livio, N. Panagia, K. Sahu. (editors), Supernovae and Gamma-Ray Bursts: The Greatest Explosions Since the Big Bang. Cambridge: Cambridge Univ. Press(2001).

[12] B. A. Harmon *et al.*, ApJS **138**, 149 (2002).

[13] D. Guetta *et al.*, Astropart. Phys. **20**, 429 (2004).

[14] K. Shinozaki and M. Teshima [AGASA Collaboration], Nucl. Phys. Proc. Suppl. **136**, 18 (2004).

[15] V. P. Egorova *et al.*, Nucl. Phys. Proc. Suppl. **136**, 3 (2004).

[16] V. Berezinsky, arXiv:astro-ph/0505220.

[17] A.V Olinto, AIP Conf. Proc. **745**, 48 (2005).

[18] P. Sommers [Pierre Auger Collaboration], arXiv:astro-ph/0507150.

[19] T. Kashti and E. Waxman, Phys. Rev. Lett. **95**, 181101 (2005).

[20] V.Berezinsky, A.Z. Gazizov and S.I. Grigorieva, Phys. Rev. **D74**, 043005 (2006).

[21] P. Meszaros, Rept. Prog. Phys. **69**, 2259 (2006) arXiv:astro-ph/0605208.

[22] V. Berezinsky, arXiv:astro-ph/0706.2158.

[23] S. Hümmer *et al.*, arXiv:astro-ph/1007.0006.

[24] R. Abbasi *et al.* [HiRes Collaboration], Phys. Rev. Lett. **100**, 101101 (2008).

[25] V. Berezinsky, arXiv:astro-ph.HE/0907.5194.

[26] K. Kotera, D. Allard and A. V. Olinto, arXiv:astro-ph/1009.1382.

[27] IceCube Collaboration, Astrophys.J. **710**, 346 (2010).

[28] R. Moharana and N. Gupta, Phys. Rev. **D82**, 023003 (2010).